A FINITE ELEMENT CODE VALIDATION FOR DYNAMIC PROBLEMS USING TIMOSHENKO BEAM THEORY AND NEWMARK ALGORITHM

Alessandro Tavares da Silva Bernardo, alebernardo@unb.br
Alessandro Borges de Sousa Oliveira, absso@unb.br
Universidade de Brasília, Faculdade de Tecnologia, Bloco C.
Departamento de Engenharia Mecânica.
Asa Norte, Brasília, DF. 70910-900

Abstract. *The purpose of this work is to validate a FE code to proceed an evaluation of dinamical response of a beam undergoing impact or dynamical loads. This code is based in the Timoshenko beam element and can calculate a dynamic evolution in time domain by Newmark scheme. The validation is made considering a cantilever beam example. The problem analytical solution is compared with two numerical simulation via FEM: (a) a modal analysis and (b) a time domain analysis of vibration response.*

Keywords: *finite element method; Timoshenko beam theory; Newmark algorithm.*

1. INTRODUCTION

Some approaches for the simulation and the study of hydrogenerators exist currently. Each one of them depends on the type of problem and on the available tools to carry on the analyses. It can be used analytical or numerical methodologies being both valid depending of course on the considered situation (Rao, 1996; Juvinal, 2000; Steidel, 1989).

One of the problems that can be present in the hydrogenarators turbines operation is the unbalancing. This type of situation might be the result of problems that occurs in assembly, manufacture, transport or the combination of some of them. These factors may cause magnetic or mass unbalancing, or both.

This work is a part of a project developed at this institution for the evaluation of the structural integrity of hidrogeradores components submitted to a magnetic unbalancing. In this project it was created a finite element code to calculate the reactions in the bearings and the proposal of wear model in these components. Hence, as it deals with magnetic forces and dynamic reactions, the problem might present non-linearity.

The aim of this work is to validate a finite element code using the Timoshenko beam theory. This code will be used for a dynamic simulation of a hydrogenarator under magnetic unbalancing. This type of problem may undergo to non-linear and non-proportional loadings, which is the reason for choosing a time-step analysis by using the Newmark algorithm.

The validation of this code will be made considering a cantilever beam situation, which the analytical solution for the natural frequencies is known. Considering this situation, the code will be used (a) to calculate the natural frequencies by numerical modal analysis and (b) to calculate the resonance frequencies by Fourier transform applied on the time-step response obtained by Newmark algorithm.

2. NUMERICAL BACKGROUND

2.1 Dynamic equation

In order to simulate situations of dynamical behavior of turbines, the ordinary differential equation in discrete dynamic problems was adopted (Zienkiewics, 1991):

$$\mathbf{M}\ddot{\mathbf{u}} + \mathbf{C}\dot{\mathbf{u}} + \mathbf{K}\mathbf{u} - \mathbf{f} = \mathbf{0}, \tag{1}$$

where $\mathbf{u}$ and $\mathbf{f}$ are, respectively, the displacement and applied force in respect to time, and $\mathbf{M}$, $\mathbf{C}$ and $\mathbf{K}$ are the mass, dumping and stiffness matrices, respectively.

2.2 Finite element model

In this work, a finite element model adopted is based on Timoshenko beam theory (Hughes, 2000; Reddy, 1993) with linear interpolation functions, i.e. an element with two nodes. The chosen element has three-dimensional displacement and three rotations, as depicted in Fig. 1a. One can see that considering a two node element (Fig. 1b) there will be six degrees of freedom for each node and twelve degrees of freedom for an element. Thus the displacement vector of an element is

$$\mathbf{u}_e = \{ u_1^1 \quad u_2^1 \quad u_3^1 \quad \theta_1^1 \quad \theta_2^1 \quad \theta_3^1 \quad u_1^2 \quad u_2^2 \quad u_3^2 \quad \theta_1^2 \quad \theta_2^2 \quad \theta_3^2 \}^T \tag{2}$$

where u_i^j and θ_i^j are respectively the displacement and rotation of node j at the direction x_i.

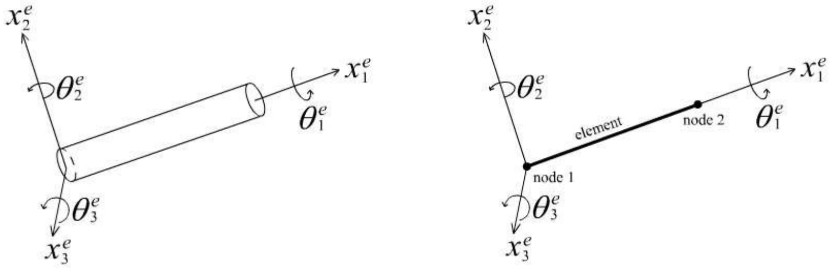

(a) (b)

Figure 1. Coordinate axis over the Timoshenko beam element.

Moreover, it will be not take into account the shear effect and will be considered a circular cross-section with radius r for the model. Gathering together all these considerations, it leads to the calculation of the element stiffness matrix as

$$\mathbf{K}_e = \begin{bmatrix}
\frac{AE}{L} & & & & & & & & & & & \\
0 & \frac{12EI}{L^3} & & & & & & & & & & \\
0 & 0 & \frac{12EI}{L^3} & & & & & & & & & \\
0 & 0 & 0 & \frac{GJ}{L} & & & & & \textit{symmetric} & & & \\
0 & 0 & -\frac{6EI}{L^2} & 0 & \frac{4EI}{L} & & & & & & & \\
0 & \frac{6EI}{L^2} & 0 & 0 & 0 & \frac{4EI}{L} & & & & & & \\
-\frac{AE}{L} & 0 & 0 & 0 & 0 & 0 & \frac{AE}{L} & & & & & \\
0 & -\frac{12EI}{L^3} & 0 & 0 & 0 & -\frac{6EI}{L^2} & 0 & \frac{12EI}{L^3} & & & & \\
0 & 0 & -\frac{12EI}{L^3} & 0 & \frac{6EI}{L^2} & 0 & 0 & 0 & \frac{12EI}{L^3} & & & \\
0 & 0 & 0 & -\frac{GJ}{L} & 0 & 0 & 0 & 0 & 0 & \frac{GJ}{L} & & \\
0 & 0 & -\frac{6EI}{L^2} & 0 & \frac{2EI}{L} & 0 & 0 & 0 & \frac{6EI}{L^2} & 0 & \frac{4EI}{L} & \\
0 & \frac{6EI}{L^2} & 0 & 0 & 0 & \frac{2EI}{L} & 0 & -\frac{6EI}{L^2} & 0 & 0 & 0 & \frac{4EI}{L}
\end{bmatrix} \tag{3}$$

where A is the circular cross-section area, E is the Young's modulus, L is the element length, G is the shear modulus, J is the torsional moment of inertia and I is the area moment of inertia.

Using the same considerations listed above, it can be found a distributed element mass matrix as

$$\mathbf{M}_e = \rho AL \begin{bmatrix}
\frac{1}{3} & & & & & & & & & & & \\
0 & m_1 & & & & & & & & & & \\
0 & 0 & m_1 & & & & & & & & & \\
0 & 0 & 0 & \frac{J}{3A} & & & & & & & & \\
0 & 0 & -m_3 & 0 & m_5 & & & & & & & \\
0 & m_3 & 0 & 0 & 0 & m_5 & & & & & & \\
\frac{1}{6} & 0 & 0 & 0 & 0 & 0 & \frac{1}{3} & & & & & \\
0 & m_2 & 0 & 0 & 0 & m_4 & 0 & m_1 & & & & \\
0 & 0 & m_2 & 0 & m_4 & 0 & 0 & 0 & m_1 & & & \\
0 & 0 & 0 & \frac{J}{6A} & 0 & 0 & 0 & 0 & 0 & \frac{J}{3A} & & \\
0 & 0 & m_4 & 0 & m_6 & 0 & 0 & 0 & m_3 & 0 & m_5 & \\
0 & -m_4 & 0 & 0 & 0 & m_6 & 0 & -m_3 & 0 & 0 & 0 & m_5
\end{bmatrix} \quad \text{where} \quad
\begin{aligned}
m_1 &= \frac{13}{35} + \frac{6}{5}\left(\frac{r_g}{L}\right)^2 \\
m_2 &= \frac{9}{70} - \frac{6}{5}\left(\frac{r_g}{L}\right)^2 \\
m_3 &= L\left[\frac{11}{210} + \frac{1}{10}\left(\frac{r_g}{L}\right)^2\right] \\
m_4 &= L\left[\frac{13}{420} - \frac{1}{10}\left(\frac{r_g}{L}\right)^2\right] \\
m_5 &= L^2\left[\frac{1}{105} + \frac{2}{15}\left(\frac{r_g}{L}\right)^2\right] \\
m_6 &= L^2\left[-\frac{1}{140} - \frac{1}{30}\left(\frac{r_g}{L}\right)^2\right]
\end{aligned} \tag{4}$$

and ρ is the specific mass of the material and $r_g = \sqrt{I/A}$ is the radius of gyration.

The damping and the gyroscopic effects will not be considered. Therefore, the term $\mathbf{C}$ of the Eq. 1 turns zero.

To solve the equation 1, it was used the Newmark algorithm, which is one of the most popular for dynamic analisys, is a time-step based and is able to calculate the dynamic response of models subjected to non-linear loads (Zienkienwics, 1991; Du et. al., 1995; Cepon et. al., 2007). This algorithm, known as the Newmark scheme, is shown in the next section.

2.3 Newmark scheme

Proceeding to the discretization of the equation 1 in a time-step scheme, considering $\Delta t = t_{n+1} - t_n$ as a time interval between the steps, it is found a new equation with the displacements and forces at the end-points of the interval:

$$\mathbf{M}\ddot{\mathbf{u}}_{n+1} + \mathbf{C}\dot{\mathbf{u}}_{n+1} + \mathbf{K}\mathbf{u}_{n+1} - \mathbf{f}_{n+1} = \mathbf{0}. \tag{5}$$

To solve this second-order problem, a quadratic expansion is the minimum requirement. Therefore considering the generic Newmark algorithm the expansion of $\dot{\mathbf{u}}_{n+1}$ and $\mathbf{u}_{n+1}$ with truncated Taylor series gives (Zienkienwics, 1991)

$$\begin{aligned}\mathbf{u}_{n+1} &= \mathbf{u}_n + \Delta t\dot{\mathbf{u}}_n + \frac{\Delta t^2}{2}(1-\beta_2)\ddot{\mathbf{u}}_n + \frac{\Delta t^2}{2}\beta_2\ddot{\mathbf{u}}_{n+1} \\ \dot{\mathbf{u}}_{n+1} &= \dot{\mathbf{u}}_n + \Delta t(1-\beta_1)\ddot{\mathbf{u}}_n + \Delta t\beta_1\ddot{\mathbf{u}}_{n+1}\end{aligned} \tag{6}$$

where β_1 and β_2 are the Newmark parameters. These, together with Eq. 5, allows the three unknowns $\ddot{\mathbf{u}}_{n+1}$, $\dot{\mathbf{u}}_{n+1}$ and $\mathbf{u}_{n+1}$ to be determined. The $\ddot{\mathbf{u}}_{n+1}$ can be obtained by substituting Eq. 6 into Eq. 5. It yields

$$\begin{aligned}\ddot{\mathbf{u}}_{n+1} = &-\left(\mathbf{M} + \mathbf{C}\beta_1\Delta t + \frac{\mathbf{K}\beta_2\Delta t^2}{2}\right)^{-1} \\ &\times\left\{-\mathbf{f}_{n+1} + \mathbf{C}\left[\dot{\mathbf{u}}_n + \Delta t(1-\beta_1)\ddot{\mathbf{u}}_n\right] + \mathbf{K}\left[\mathbf{u}_n + \Delta t\dot{\mathbf{u}}_n + \frac{\Delta t^2}{2}(1-\beta_2)\ddot{\mathbf{u}}_n\right]\right\}.\end{aligned} \tag{7}$$

After the calculation of $\ddot{\mathbf{u}}_{n+1}$, the values of $\dot{\mathbf{u}}_{n+1}$ and $\mathbf{u}_{n+1}$ can be found using the equations 6.

The choice of Newmark parameters, β_1 and β_2, play a important role in stability of the algorithm. The unconditional stability can be achieved by adopting (Zienkiewics, 1991)

$$\beta_1 \geq \beta_2 \geq \tfrac{1}{2}. \tag{8}$$

However, some authors adopt the values $\beta_1 = \frac{1}{2}$ and $\beta_2 = \frac{1}{4}$ to obtain the second-order accuracy (Brank et. al., 2003).

2.4 Fast Fourier transform (FFT)

In the previous section was presented a Newmark algorithm, which is able to evaluate the dynamic evolution of the displacements, i.e. presents the results of dynamic response over the time domain. However the validation of the FE model developed in this work is only possible at frequency domain due to the existence of analytical solutions for modal analysis (Steidel, 1989). To proceed the transformation from time domain to frequency domain, it was applied the *fast Fourier transform* algorithm (FFT) onto the discrete time-step results (Oppenhein et. al., 1989; Bendat et. al., 1989). The application of this algorithm in a local displacement u_n, where n is the time-step index varying from 1 to N (the total steps in time), yields the expression

$$p_k = \sum_{n=1}^{N} u_n e^{\frac{-2i\pi nk}{N}}, \tag{9}$$

where the values of p_k are the amplitudes in frequency domain. To plot graphs of amplitude versus frequency in hertz, the corresponding abscissa can be obtained by $\frac{k}{N\Delta t}$.

3. VALIDATION OF FE CODE

A finite element code was developed using a free software called Scilab (2007). To validate the code it was chosen three situations that have well documented analytical solutions of the modal analysis (Steidel, 1989). These solutions will be compared to numerical solutions. These situations are: longitudinal (Fig. 2a), transverse (Fig. 2b) and torsional (Fig. 2c) non-forced free vibration of a cantilever beam with a circular cross-section. The material and geometrical properties used for the validation are:

$$E = 200GPa, \quad \nu = 0.3, \quad \rho = 7850 kg/m^3, \quad r = 0.05m, \quad and \quad L = 0.9m, \tag{10}$$

where ν is the Poisson ratio, r is the circular cross-section radius and L is the length of the beam.

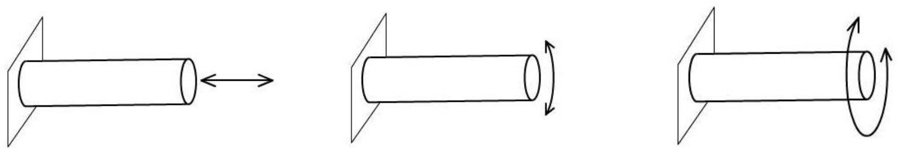

Figure 2. Cantilever beam and the three situations of vibration.

3.1 Analytical solution

The analytical solutions for the situations depicted above (Fig. 2) are presented into wave differential equations (Steidel, 1989). Moreover, the calculation of natural frequencies for some geometries considering simple boundary conditions and free vibration are straightforward.

The solutions for the natural frequencies for the first three modal vibrations are:

$$f_1^{lon} = \frac{1}{4L}\sqrt{\frac{E}{\rho}}, \quad f_2^{lon} = \frac{3}{4L}\sqrt{\frac{E}{\rho}}, \quad and \quad f_3^{lon} = \frac{5}{4L}\sqrt{\frac{E}{\rho}} \quad \text{for longitudinal vibration;} \tag{11}$$

$$f_1^{tra} = \frac{0.5595}{L^2}\sqrt{\frac{EI}{\rho A}}, \quad f_2^{tra} = \frac{3.5069}{L^2}\sqrt{\frac{EI}{\rho A}} \quad and \quad f_3^{tra} = \frac{9.8203}{L^2}\sqrt{\frac{EI}{\rho A}} \quad \text{for transverse vibration;} \tag{12}$$

$$f_1^{tor} = \frac{1}{4L}\sqrt{\frac{G}{\rho}}, \quad f_2^{tor} = \frac{3}{4L}\sqrt{\frac{G}{\rho}}, \quad and \quad f_3^{tor} = \frac{5}{4L}\sqrt{\frac{G}{\rho}} \quad \text{for torsional vibration.} \tag{13}$$

These equations 11, 12 and 13 with the validation values (10) yield the results in table 1.

Table 1. Results of analytical solution.

Longitudinal vibration	Transverse vibration	Torsional vibration
$f_1^{lon} = 1402{,}1Hz$	$f_1^{tra} = 87{,}165Hz$	$f_1^{tor} = 869{,}54Hz$
$f_2^{lon} = 4206{,}3Hz$	$f_2^{tra} = 546{,}34Hz$	$f_2^{tor} = 2608{,}6Hz$
$f_3^{lon} = 7010{,}5Hz$	$f_3^{tra} = 1529{,}9Hz$	$f_3^{tor} = 4347{,}7Hz$

3.2 Modal analysis with FE model

The calculation of the natural frequencies by a modal analysis via finite element analysis for the situations depicted in Fig. 2 considering no damping nor gyroscopic effect is easy when the response function of the vector of nodal global displacements is considered as

$$\mathbf{u}_m(t) = \mathbf{a}\sin(2\pi f t) + \mathbf{b}\cos(2\pi f t) \tag{14}$$

where $\mathbf{a}$ and $\mathbf{b}$ are amplitude vectors, f is the vibration frequency and t is the time. Moreover, substituting the function $\mathbf{u}_m(t)$ (Eq. 14) into $\mathbf{u}$ of the movement equation (Eq. 1) with $\mathbf{C} = \mathbf{0}$ and $f = \mathbf{0}$ (non-forced vibration), it is obtained

$$\ddot{\mathbf{u}}_m(t) = -(2\pi f)^2 \mathbf{u}_m(t) \quad \text{and} \quad (\mathbf{K}^{-1}\mathbf{M})\mathbf{u}_m = \frac{1}{(2\pi f)^2}\mathbf{u}_m , \tag{15}$$

which is an eigenvalues problem where the biggest eigenvalue leads to calculation of a natural frequency of a first vibration mode, the second biggest leads to calculation of a natural frequency of a second vibration mode and so on. It was adopted the finite element model shown in the Section 2, i.e. the element vectors and matrixes showed in 2, 3 and 4 (Timoshenko beam element with two nodes) was considered. The FE mesh is homogeneous, has the orientation depicted in Fig. 3 and present q elements, which will be chosen by proceeding a convergence analysis.

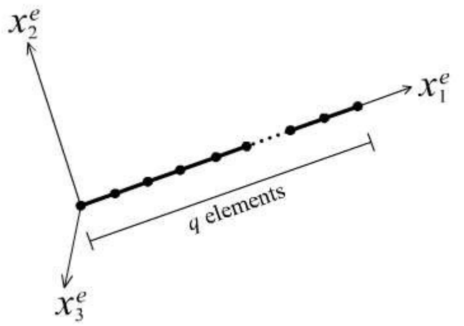

Figure 3. Mesh orientation.

The convergence analysis consists in the calculation of the third longitudinal vibration mode by FE analysis and the comparison of the results with the analytical solution $f_3^{lon} = 7010{,}5Hz$ (Tab. 1). A variation of the element number q was made, the eigenvalue problem (Eq. 15) was mounted and the natural frequencies were calculated. The results are shown in table 2. It was observed during this analysis that the considered mode (third longitudinal mode) is the sixteenth mode in the implemented FE model.

Table 2. Mesh convergence analysis results.

Number of mesh elements q	Natural frequency by FE analysis (Hz)
10	7191.8
20	7055.6
40	7021.7
80	7013.3
160	7013.3

The difference of mesh results with $q = 40$ compared to $q = 160$ is less than 0.12%. Therefore the chosen value for q is 40. With this result the validation procedures can proceed.

Considering the mesh (Fig. 3) with $q = 40$, the FE analysis will be made by calculating the eigenvalues problem of Eq. 15 and comparing the modal shapes with the known ones (Steidel, 1989). It can be noted that the results of the numerical calculation will lead to two values of natural frequency of transverse vibration mode (along x_2 and x_3). It will be considered only value along x_2 for comparison to analytical results (Tab. 1).

Proceeding to this modal analysis via finite element it was achieved the values and the number of the corresponding mode showed in Table 3. The figures 4, 5 and 6 depict the modal shapes of longitudinal, transverse and torsional vibrations, respectively.

Table 3. Modal analysis via finite element.

Mode	Natural frequencies (Hz)	Type of vibration and corresponding shape.
1st	87.023	1st transverse mode (Fig. 5a)
3rd	539.63	2nd transverse mode (Fig. 5b)
5th	869.60	1st torsional mode (Fig. 6a)
6th	1402.2	1st longitudinal mode (Fig. 4a)
7th	1486.1	3rd transverse mode (Fig. 5c)
9th	2610.1	2nd torsional mode (Fig. 6b)
12th	4208.7	2nd longitudinal mode (Fig. 4b)
13th	4344.7	3rd torsional mode (Fig. 6c)
20th	7021.7	3rd longituinal mode (Fig. 4c)

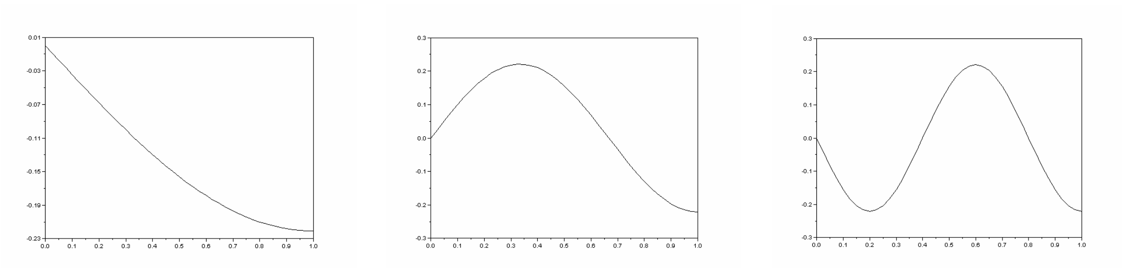

(a) (b) (c)

Figure 4. Longitudinal vibration: (a) mode 1, (b) mode 2 and (c) mode 3.

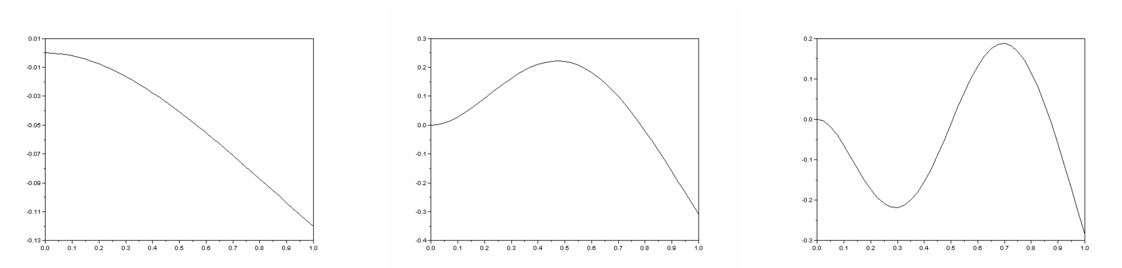

(a) (b) (c)

Figure 5. Transverse vibration: (a) mode 1, (b) mode 2 and (c) mode 3.

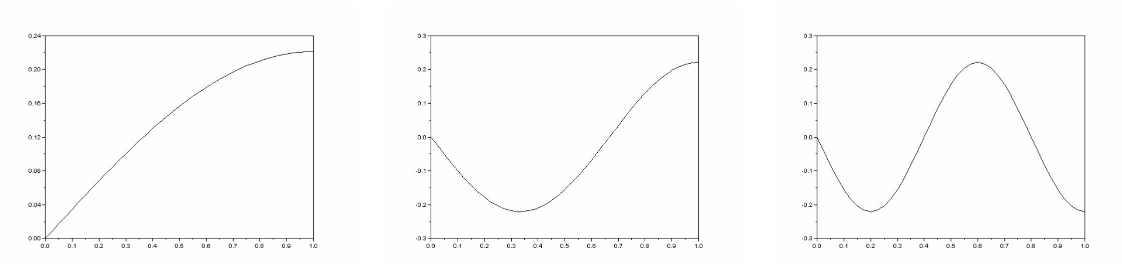

(a) (b) (c)

Figure 6. Torsional vibration: (a) mode 1, (b) mode 2 and (c) mode 3.

3.3 Time-step analysis with FE model

In order to proceed this analysis, it was considered the same mesh adopted in the previous section (Fig. 3, uniform mesh and $q = 40$). The basic idea of such analysis is to apply an impulse force at the endpoint of the FE mesh (the free node), i.e. impose a unitary force at this node only at the first step of time. Then it is registered the time vibration response of this node. This response is periodic and the FFT algorithm is used. The result of the

FFT is a frequency domain graphic, which the picks correspond to the resonance frequencies. These picks values can be related to the natural frequencies because no damping was considered in the FE model.

The analysis was made separately, considering the three situations showed in Fig. 2. In each analysis, a number of time steps N, a time interval Δt and a unitary impulse to the required excitation (longitudinal, transverse and torsional). The results of time-step simulation and FFT are depicted in figures 7, 8 and 9. Table 3 show the problem parameters and resonance frequencies obtained by graphical analysis. It was selected the Newmark parameters as $\beta_1 = \beta_2 = 1/2$.

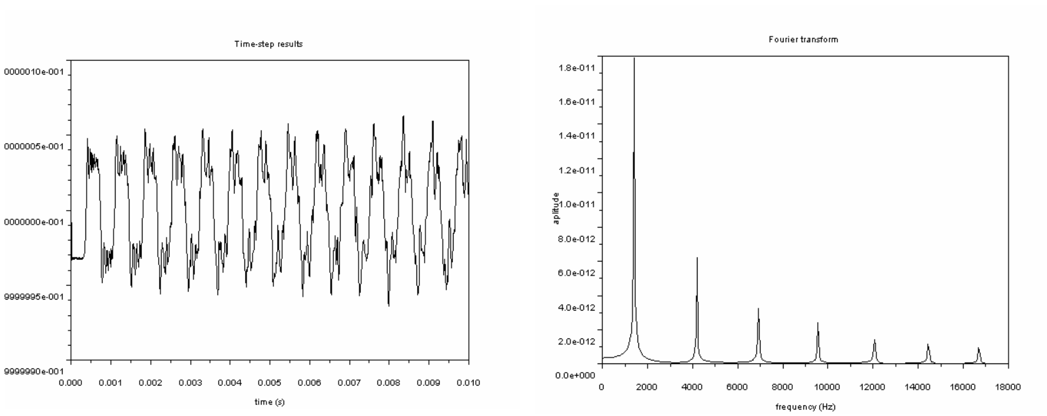

(a) (b)

Figure 7. Longitudinal vibration using $N = 2098$ and $\Delta t = 10^{-5} s$: (a) endpoint response and (b) corresponding FFT.

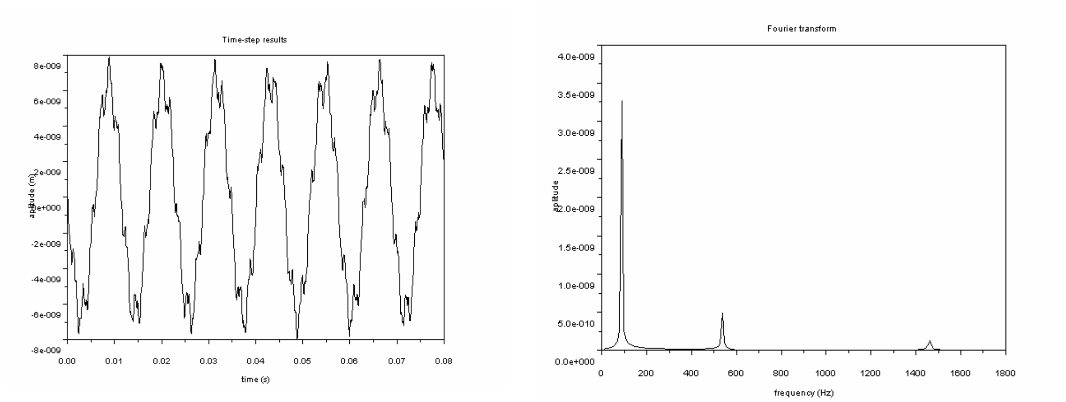

(a) (b)

Figure 8. Transverse vibration using $N = 2098$ and $\Delta t = 5 \cdot 10^{-5} s$: (a) endpoint response and (b) corresponding FFT.

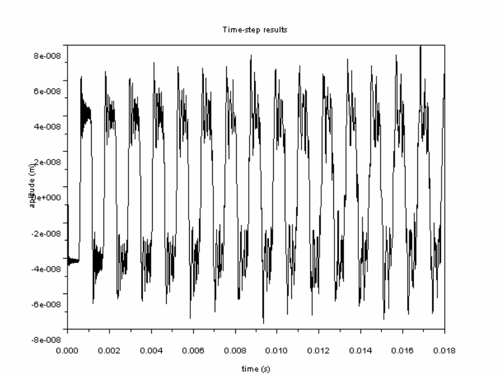

(a)

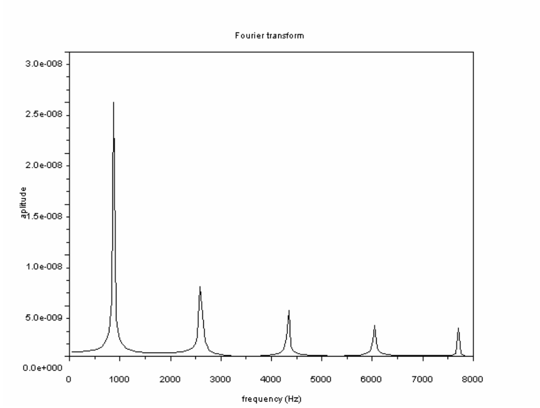

(b)

Figure 9. Torsional vibration using $N = 2098$ and $\Delta t = 10^{-5} s$: (a) endpoint response and (b) corresponding FFT.

Table 4. Resonance frequencies in the three chosen situations.

Vibration type	Δt (s) Time step	N Quantity of steps	Frequencies by FFT picks (Hz)	
Longitudinal	$1 \cdot 10^{-5}$	2098	1st	1416
			2nd	4197
			3rd	6930
Transverse	$5 \cdot 10^{-5}$	2098	1st	87.85
			2nd	536.9
			3rd	1464
Torsional	$1 \cdot 10^{-5}$	2098	1st	878.5
			2nd	2587
			3rd	4344

3.4 Analytical solution versus Natural frequencies and FFT results

The results were compared with each other considering the analytical as a reference. This assessment can be numerically seen in table 5, that shows that the biggest relative difference is 4.31%, which corresponds to the transverse vibration.

Table 5. Differences between the results.

	Relative difference in relation to analytical solution (%)			
Vibration type	Modal analysis by FE analysis		Time-step FE analysis and FFT	
Longitudinal	1st	< 0.01	1st	0.96
	2nd	0.02	2nd	0.22
	3rd	0.16	3rd	1.15
Transferse	1st	0.16	1st	0.79
	2nd	1.23	2nd	1.73
	3rd	2.86	3rd	4.31
Torsional	1st	< 0.01	1st	1.03
	2nd	0.06	2nd	0.85
	3rd	0.07	3rd	0.10

4. CONCLUSION

Considering the FE code produced, one can notice the beam theory and the mesh adopted (table 5) with the application of FFT over the Newmark scheme results provide results very close to the analytical solution considering a cantilever beam. This set of choices and considerations composes a model able to simulate the simple considered situation.

This code has been successfully used in this institution to simulate an hydrogenerator dynamic response considering any type of unbalancing. It is much more complex that the problem showed in this paper. Moreover there is no previous solution that can be used to comparison. However this work verified that this code is able to calculate a time-step evolution by FE method. To a complex problem such as hydrogenerator situations, the appropriate boundary and initial conditions has to be chosen together with the application of the unbalanced loads predicted by the magnetic theories.

5. ACKNOWLEDGEMENTS

The authors acknowledge ELETRONORTE for supporting this work.

6. REFERENCES

Bendat, J.S. and Pierson, A.G. Random data: analysis and measurement procedures. 2nd ed. Wiley, New York, 1989.
Brank, B., Korelc, J. and Ibrahimbegovic, A. Dynamics and time-stepping schemes for elastic shells undergoing finite rotations. Computers & Structures 81, pp. 1193-1210. 2003.
Cepon, G. and Boltezar, M. Computing the dynamic response of an axially moving continuum. Journal of Sound and Vibration 300, pp. 319-329. 2007.
Du, H. and Ling, S. F. A nonlinear dynamics model for three-dimensional flexible linkages. Computers & Structures. Vol. 56. No. 1. pp. 15-23. 1995.
Hughes, T.J.R. The Finite Element Method: linear static and dynamic finite element analysis. Dover publications, New York, 2000.
Juvinall, R.C. and Marshek, K.M. Fundamentals of Machine Component Design. 3rd ed. John Wiley & Sons, 2000.
Oppenheim, A.V. and Schafer, R.W. Discrete-time Signal Processing. Prentice Hall, New Jersey, 1989.
Reddy, J.N. An Introduction to the Finite Element Method. McGraw-Hill, 1993.
Rao, J.S. Rotor Dynamics. 3rd ed. New Age International, New Delhi, 1996.
Scilab 4.1. Online help. 21 April 2007 <http://www.scilab.org/product/man-eng/index.html>.
Steidel, R.F. An Introduction to Mechanical Vibrations. Wiley, New York, 1989.
Zienkiewics, O.C. and Taylor, R.L. The Finite Element Method, Vol. 2. 4th ed. McGraw-Hill, England, 1991.

7. RESPONSIBILITY NOTICE

The authors are the only responsible for the printed material included in this paper.